CLM-P380

This document is intended for publication in a journal, and is made available on the understanding that extracts or references will not be published prior to publication of the original, without the consent of the authors.

CLM-P380

FUSION LIBRARY
CULHAM
13 DEC 1996
b

UKAEA RESEARCH GROUP

Preprint

INTERACTION BETWEEN TWO COLLIDING LASER PRODUCED PLASMAS

P T RUMSBY
J W M PAUL
M M MASOUD

CULHAM LABORATORY
Abingdon Berkshire

1974

Enquiries about copyright and reproduction should be addressed to the
Librarian, UKAEA, Culham Laboratory, Abingdon, Berkshire, England

CLM - P 380

INTERACTIONS BETWEEN TWO COLLIDING LASER PRODUCED PLASMAS

by

P.T. Rumsby *, J.W.M. Paul and M.M. Masoud ≠

(Submitted for publication in Plasma Physics)

ABSTRACT

We have observed two types of interaction between two adjacent expanding plasmas, produced by laser irradiation. The density and temperature of both the initial and interacting plasmas have been measured by photon scattering. For interaction early in the expansion the results can be explained by classical ion-ion collisions, while for later interaction (lower density) electron-electron and electron-ion collisions provide an explanation.

* Also at Department of Engineering Science
Oxford University.

≠ Dept. of Physics & Physical Electronics,
Newcastle-upon-Tyne Polytechnic.

UKAEA Research Group,
Culham Laboratory,
Abingdon,
BERKS.

January, 1974

CONTENTS

		Page
1.	INTRODUCTION	1
2.	SINGLE PLASMA RESULTS	2
3.	MODEL FOR CASE A	3
4.	RESULTS AND INTERPRETATION FOR CASE 'A'	5
5.	MODEL FOR CASE 'B'	7
6.	RESULTS AND INTERPRETATION FOR CASE 'B'	8
7.	CONCLUSION	9
	ACKNOWLEDGEMENTS	10
	REFERENCES	10

1. INTRODUCTION

When two streaming plasmas collide various interactions can arise. These may be of collisionless type in which collective plasma effects occur (BABYKIN et al, 1963; LITTLE,, et al, 1970) or collision dominated (PUELL et al, 1970a; KOOPMAN, 1972).

We have investigated experimentally the interactions that occur when two laser produced plasmas collide. Fig.1 shows the arrangement used to produce the two plasmas. A pulse (4.5 J, 45 ns) from a Nd-glass laser is split into two beams which are focused onto adjacent spots (dia. ~250 μm) on a carbon plate in vacuum. The resulting plasmas expand away from the target but into each other in a direction parallel to the target surface.

Two distinctly different interactions can be seen on framing camera pictures (Fig.2) taken from a direction perpendicular to the plane of the two laser beams.

CASE A When the focal spot separation d = 10 mm, the interaction region is seen as a strongly luminous band 2-3 mm wide (Fig.2(a)).

CASE B When d = 40 mm a larger interaction region is observed which is less luminous than the surrounding regions of unperturbed plasma. (Fig.2(b)).

We present measurements of both electron density and temperature and then use these to explain the two interactions in terms of classical binary collisions.

2. SINGLE PLASMA RESULTS

To establish the initial conditions for the interaction, we have measured the density of a single expanding plasma at various distances along the target normal (x-direction) and also at 45^{o} to this direction. The measurements, made with a charge collecting probe, have shown a shell like structure, which expands at constant velocity. The front of the shell expands in the x-direction at a velocity $V_{\perp} = 130\,km\,s^{-1}$ (1.06 keV) while the peak density has $\bar{V}_{\perp} = 100\,km\,s^{-1}$ (625 eV). The corresponding velocities in the 45^{o} directions are $V_{45} = 92\,km\,s^{-1}$ (530 eV) and $\bar{V}_{45} = 64\,km\,s^{-1}$ (256 eV). Thus the region of peak shell density travelling at 45^{o} to the target normal has a y component of velocity given by $(\bar{V}_{45})_{y} = 45\,km\,s^{-1}$ (126 eV). As shown in Fig.1, the plasma behaves very nearly like an expanding hollow sphere touching the target surface,

The peak electron density in the shell (n_{eo}) and the corresponding electron temperature (T_{eo}) have been measured by photon scattering using ruby laser light. The experimental arrangement has been described fully elsewhere (RUMSBY and PAUL, 1974). The results are shown in Fig.3 together with density measurements made with the charge collecting probe. These results are in agreement with our published study (RUMSBY and PAUL, 1974) of a similar expanding laser produced plasma, e.g. $n_{e} \propto r^{-3}$ while $T_{e} \propto r^{-1}$ as a consequence of the heating effects of three body recombination.

The ionic charge Z of an expanding laser produced plasma can be predicted from the theory of PUELL (1970b). For the radiation power density involved here ($\sim 10^{15}$ watts. m^{-2}) the expanding ions in the shell would be expected to have $Z \sim 2$ or 3.

3. MODEL FOR CASE A

With $d = 10\,mm$ the two shells first collide along the 45^{o} line at $x = 5\,mm$. The initial plasma conditions before interaction have been obtained by extrapolating the single plasma measurements of $n_{eo}(45)$ and $T_{eo}(45)$ given in Fig.3. The deduced parameters are listed in Table 1. The table also shows the calculated values of the ion-ion mean free path (λ_{i1}) for interstreaming parallel to the target surface (y-direction). These are sufficiently small to cause appreciable momentum transfer between the interpenetrating plasmas. The relative velocity of the plasmas will be reduced by the interaction and the momentum transfer cross-sections increased. We expect a rapid build-up of stationary plasma in the interaction region.

The two plasma flows will interact with a relative Mach number $M_s \sim 3$, and consequently produce two oppositely directed ($\pm y$) gas dynamic shocks. For sufficiently strong shocks, and $\gamma = 5/3$ the compression ratios will approach 4. Particle flux continuity across the shock then dictates that the laboratory shock velocity approaches 1/3 the incoming plasma flow velocity, i.e. $V_s = 15\,km\,s^{-1}$. This gives a shock Mach number ~ 4. As the post shock plasma is stationary in the laboratory frame all the directed plasma flow energy will be converted to thermal ion energy behind the shock ($T_i \sim 86\,eV$) giving an ion-ion mean free path, $\lambda_{i2} \sim 0.3\,mm$ ($\tau_i \sim 5\,ns$). The shock thickness should be of this order, (JUKES, 1957).

The thermal ion energy of the hot plasma between the two shock waves will be converted back into directed ion energy as the plasma expands preferentially in the x and z directions. Such a model of two separating shock waves with stationary hot dense plasma between

is applicable only up to the time that the rear of the expanding plasma shells reach the outgoing shock waves ($t \sim 0.35\ \mu s$).

TABLE 1

PLASMA PARAMETERS BEFORE AND AFTER INTERACTION

		CASE A	CASE B
	d mm	10	40
	r mm	7	28
	x mm	5	20
Initial Plasma Parameters	n_{eo} m^{-3}	2×10^{22} *	2.8×10^{20}
	T_{eo} eV	1.4 *	0.37
Calculated λ_{i1} mm	Z = 2	6	400
	Z = 3	1.6	107
Interacting Region Parameters	n_e , m^3	1×10^{23} ≠	6×10^{20}
	$\frac{n_e}{n_{eo}}$ measured	5 ≠	2
	$\frac{n_e}{n_{eo}}$ expected	3.5 - 4	2
	T_e eV	~ 7 ≠	3.1
	$\frac{T_e}{T_{eo}}$ measured	~ 5 ≠	8.4
	$\frac{T_e}{T_{eo}}$ expected	~2.5 (adiabatic compression only)	8 - 10

*extrapolated from single plasma measurements n_{eo} (45°) and T_{eo} (45°) from Fig.3.

≠ extrapolated from interaction region measurement made at x = 10 , 15 and 20 mm (Fig.4).

4. RESULTS AND INTERPRETATION FOR CASE 'A'

We now show that the experiment is in agreement with the above model. The measurements can be summarized as follows:

(a) The interaction zone is 2 to 3 mm wide and does not change appreciably during its life of 0.1 μs .

(b) Photon scattering measurements within the interaction zone at $x = 10$, 15 and 20 mm and peak shell density yield (Fig.4)

(i) $n_e \approx 5\, n_{eo}$

(ii) $T_e \approx 5\, T_{eo}$

(c) Measurements with the charge collecting probe show that at 100 mm along the target normal through the interaction zone, the mean ion expansion energy in that direction is 730 eV which is 105 eV greater than for a single plasma.

Table 1 lists the deduced plasma parameters at $x = 5$ mm , extrapolated from Fig.4.

An increase in electron density by a factor 5 is consistent with the predicted ion density jump of about 4 across the shock and some ionization behind the shock to give an increase in average z of about 25%. We show below that this is a reasonable assumption. For our model, in the interaction region $T_i \sim 86$ eV $\gg T_e \sim 7$ eV . This low value of electron temperature is consistent with adiabatic compression plus a slow energy transfer from the ions to the electrons ($T_{eq} \sim 0.1$ μs) making allowance for the free expansion of the ions in the x and z directions. The observed increase in expansion energy in the x direction is consistent with the 126 eV lost in the y direction as would be expected for the model proposed.

The fact that the width of the strongly luminous interaction region changes little in 0.1 μs is consistent with the low shock velocities (15 km.s^{-1}) expected in the y-direction.

Interpretation of the framing camera photographs is complicated by the fact that they represent integrations over the large spectral range of an S-20 photocathode. However it is possible to make qualitative statements about the relative intensities of light emitted by the various plasma regions.

Bates et al (1962) have calculated plasma collisional-radiative recombination and ionization coefficients for ions (assumed hydrogenic) of arbitrary charge Z. From their results we may calculate recombination rates (R_R) and ionization rates (R_I) for a particular ion species, assuming that the plasma consists predominantly of the one species with density $n_i = \frac{n_e}{Z}$. We conclude that for the deduced initial plasma parameters occurring before interaction and any given ion species with $Z = 1, 2$ or 3, $R_{I_1} \ll R_{R_1}$, i.e. ionization is negligible compared with recombination. For the deduced parameters of the denser hotter plasma in the interaction region the rates are changed such that for species with $Z = 1$ or 2 $R_{I_2} > R_{R_2} \gg R_{I_1}$, while for $Z = 3$ we always have $R_{I_2} < R_{R_2}$. Thus we expect ionization to occur when the two plasmas interact if the plasmas consist of ions with $Z = 1$ or 2. The values involved correspond to rapid ionization in less than 0.1 μs, and thus would explain the above 25% increase in average Z.

In such a situation, we expect the majority of light detected by the camera to be due to line radiation (PUELL, 1970b) and consequently the increase in ionization due to the increased density and

temperature will give rise to enhanced light output from the interaction region as observed.

STRINGER (1964) has calculated under what conditions of drift velocity and ion-electron temperature ratio instabilities occur when two hydrogen plasmas interstream. We have generalized these results to treat the case of two interstreaming carbon plasmas. Initially the two plasmas collide with $T_e/T_i = 1$ and $V_y/C_s \sim 3$ giving a system stable to both ion-ion and ion-electron instabilities. As interaction proceeds T_e/T_i reduces to about 0.1 and V_y/C_s reduces to about 0.3. We conclude that the system always remains stable.

5. MODEL FOR CASE 'B'

Table 1 lists the pre-interaction parameters occurring when the two plasmas first meet at $x = 20\,mm$. The calculated values of λ_{i1} for interstreaming in the y-direction are now very large. The ions are thus collisionless and interstreaming of the two plasmas occurs. The interstreaming electron gases are highly collisional ($\lambda_{ee} \sim 2 \times 10^{-3}\,mm$) and hence rapidly form a stationary cold electron background. The ions continue to interstream through this background heating the electrons by electron-ion collisions. Using Spitzer's expression for the rate of loss of ion energy (ROSE and CLARK, 1961) we estimate that the electron temperature should rise by 3 to 4 eV as the two plasma shells pass through each other. Clearly the density in the interacting region is simply twice that for a single plasma.

6. RESULTS AND INTERPRETATION FOR CASE 'B'

The experimental results can be summarized as follows:

(a) The interaction region is dark on the framing pictures and expands with time corresponding with the overlap region of the two expanding plasmas.

(b) Photon scattering measurements at $t = 20, 30, 40\,mm$ in the interaction region when the two shell peaks overlap show: (Fig.5)

$$(i) \quad n_e = 2\, n_{eo}$$

$$(ii) \quad T_e \sim 8\, T_{eo} .$$

Table 1 lists the measured plasma parameters at $x = 20\,mm$.

The framing camera pictures and the doubling of the density confirm the model based on collisionless ion inter-streaming. The measured electron temperature is in close agreement (Table 1) with the predicted collisional heating by the ions.

As for case 'A' we have calculated the ionization and recombination rates. Before the two plasma collide at $x = 20\,mm$, recombination dominates ionization ($R_{R_1} \gg R_{I_1}$) for a plasma consisting of ions with $Z = 1, 2$ or 3. After interaction for plasmas consisting of ions with $Z = 2$ or 3 ionization remains unimportant ($R_{R_2} \gg R_{I_2}$) but the recombination rate is typically one or two orders of magnitude less than its pre-interaction value ($R_{R_2} \ll R_{R_1}$) leading to a reduction in the cascade type line radiation emitted by ions or atoms after electron capture into high levels. This is consistent with the observed reduction in light emitted from the interaction region (Fig.2). However if the plasma consists of ions with $Z = 1$, then after the

interaction $R_{I_2} > R_{R_2} > R_{I_1}$ and ionization would occur as discussed in case 'A'.

Comparing the light output models of case 'A' and 'B' one sees that they are consistent only if the plasma consists of ions with $Z = 2$. Most of the framing camera photographs are taken after the shell peaks collide ($t = 0.11\ \mu s$ for Case 'A', $0.45\mu s$ for Case 'B'). Such a value of Z is reasonable for the rear of the shells.

When the two plasmas first collide with $T_e/T_i = 1$ and $V_y/C_s \sim 5$ we deduce that no streaming instabilities should occur. (STRINGER 1964). Even at later times in the interaction as the electrons are collisionally heated and T_e/T_i increases from 1 to about 8 we conclude that the system should remain stable.

7. CONCLUSION

We have measured the plasma parameters occurring in the interaction region when two laser produced plasmas collide. The measurements of density and temperature are entirely consistent with proposed models based on (a) classical ion-ion collisions for interaction early on when the plasmas have high density and (b) electron-electron and electron-ion collisions for interaction at later times when the densities are much lower.

We have concluded that when the two plasmas collide at high density rapid collisional ionization occurs leading to an enhancement in the observed luminosity. For the lower density interaction however ionization never becomes important and recombination remains dominant. However, recombination is at a much lower rate than before interaction, leading to a reduction in the observed luminosity.

ACKNOWLEDGEMENTS

The authors wish to acknowledge the encouragement and advice given by Dr R.J. Bickerton.

REFERENCES

BABYKIN, M.V., ZAVOISKII, E.K., RUDAKOV, L.I. and SKORYUPIN, V.A. (1963), Sov. Phys. J E T P , 16, 1391.

BATES, D.R., KINGSTON, A.E., and McWHIRTER, R.W.P., (1962) Proc. R. Soc., Lond., A267, 297.

JUKES, J.D., (1957), J. Fluid Mechs., 3, 275

KOOPMAN, D.W., (1972), Phys. Fluids, 15, 1959.

LITTLE, P.F., AVIS, B.E. and TURNER, R.B., (1970), Plasma Physics, 12, 565.

PUELL, H., OPOWER, H. and NEUSSER, H.J., (1970a), Phys. Letts., 31A, 4.

PUELL, H., (1970b), Z. Naturforsch, 25a, 1807.

ROSE, D.J. and CLARK, M.C., (1961), 'Plasma and Controlled Fusion', M I T Press.

RUMSBY, P.T. and PAUL, J.W.M., (1974), Plasma Physics, 16 , 247

STRINGER, T.E., (1964), Plasma Physics, 6, 267.

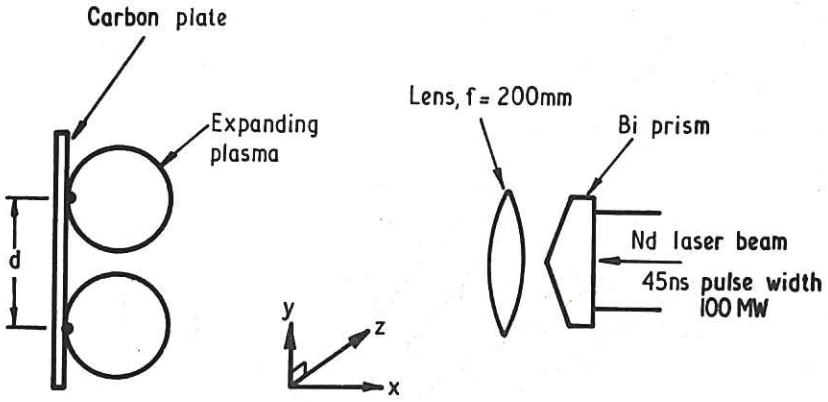

Fig. 1. Experimental arrangement

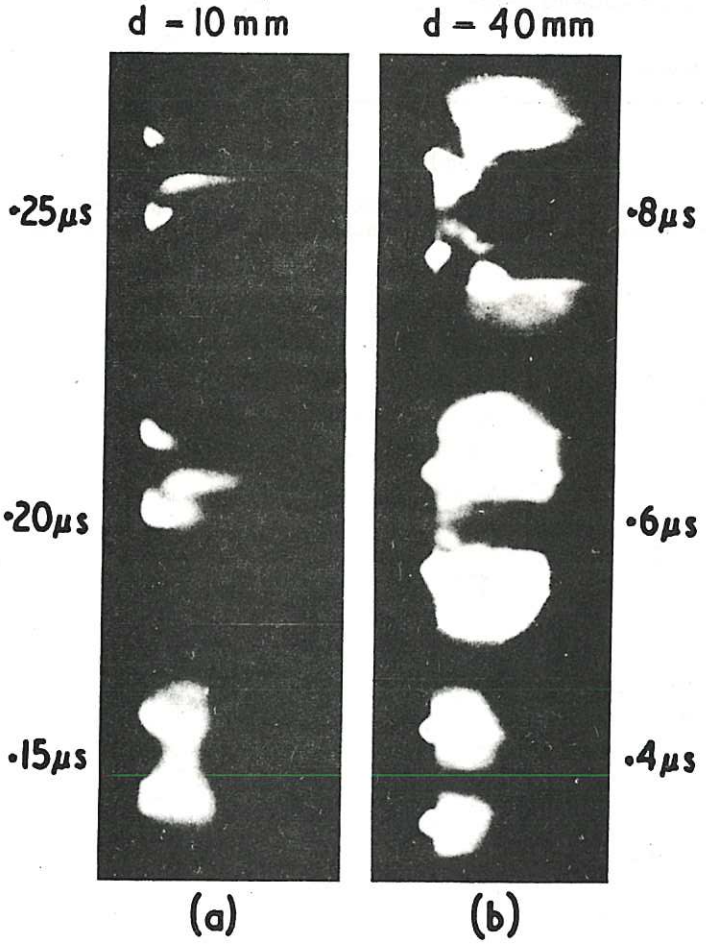

Fig. 2. Framing camera photographs of the interactions
(a) CASE A, spot separation d = 10 mm aperture f/8, 5 ns exposure;
(b) CASE B, spot separation d = 40 mm aperture f/2, 20 ns exposure.

CLM-P 380

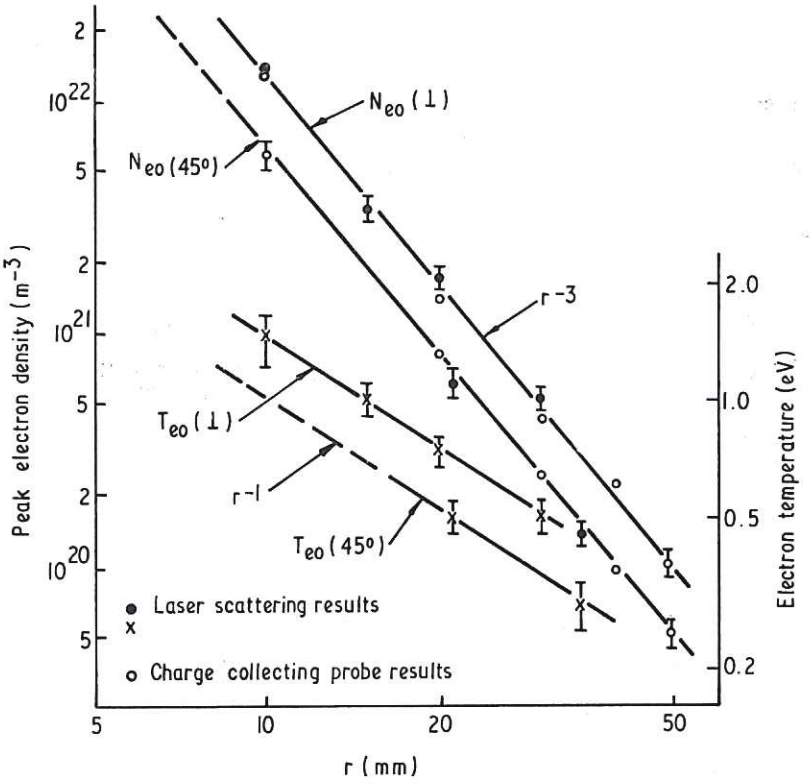

Fig. 3. Single expanding plasma shell peak density and temperature for expansion along target normal (1) and Expansion at 45° to target normal (45°).

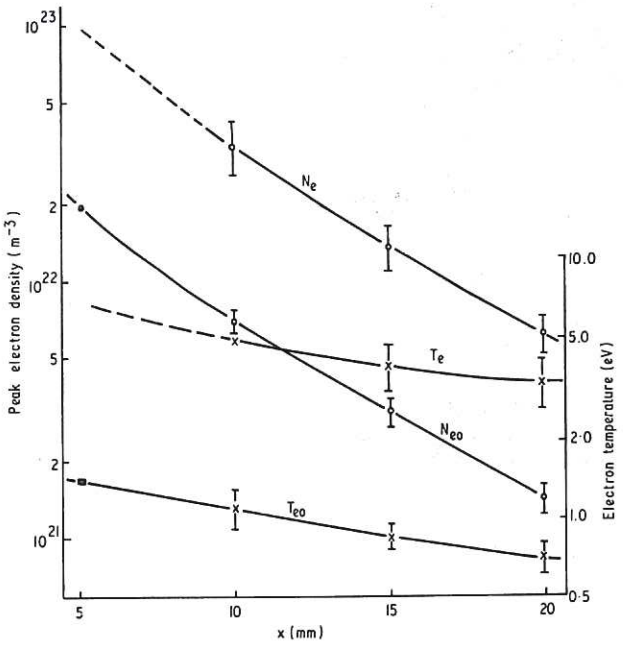

Fig. 4. CASE A, interaction region density and temperature measurements.
Interacting plasma parameters - n_e, T_e.
Single plasma parameters - n_{eo}, T_{eo}.
Data points at x = 5 mm obtained by extrapolation from Fig. 3.

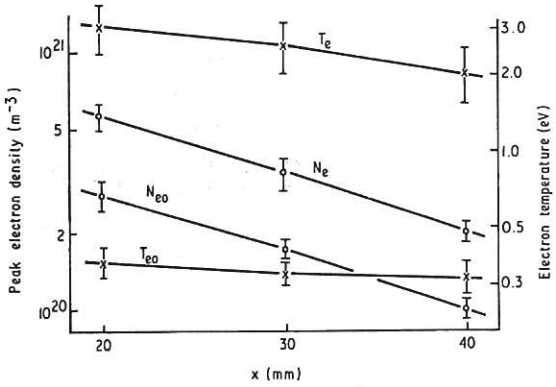

Fig. 5. CASE B, interaction region density and temperature measurements.
Interacting plasma parameters - n_e, T_e.
Single plasma parameters - n_{eo}, T_{eo}.